

High-pressure Raman study of one-dimensional crystals of the very polar molecule hydrogen cyanide

K. Aoki,* B. J. Baer, H. C. Cynn, and M. Nicol

Department of Chemistry and Biochemistry, University of California, Los Angeles, Los Angeles, California 90024-1569
(Received 26 February 1990)

At ambient temperature, hydrogen cyanide freezes at 0.2 GPa and undergoes a solid-solid transition at 0.8 GPa. Compression beyond 1.3 GPa induces polymerization. The crystal structures stable between 0.2 and 0.8 GPa and above 0.8 GPa were identified as the body-centered tetragonal and orthorhombic structures, respectively, that also occur at low temperatures and ambient pressure. Both structures consist of linear chains of molecules aligned parallel to the c axis of the unit cell. The Raman peak for the internal C—H stretching mode shifts to lower frequency with increasing pressure in both solid phases because compression strengthens the intrachain hydrogen bond. The frequency of the Raman-active libration increases rapidly with increasing pressure in the tetragonal phase and at an even greater rate in the orthorhombic phase. The LO-TO splitting of the librational mode, $\omega_{LO}-\omega_{TO}$, decreases monotonically with increasing pressure, whereas the difference between the squares of these frequencies, $\omega_{LO}^2-\omega_{TO}^2$, is independent of pressure.

INTRODUCTION

Hydrogen cyanide, HCN, is a linear polar molecule with a C \equiv N triple bond. In crystals of pure hydrogen cyanide, the molecules are aligned head to tail by H—C \equiv N \cdots H—C \equiv N hydrogen bonds. Two crystalline phases are known at ambient pressure: a tetragonal phase from the normal melting point, 260–170 K and an orthorhombic phase at lower temperatures.^{1,2} Both structures are body centered with two molecules per unit cell and, more important for Raman spectroscopy, one molecule per primitive cell. The structure of the tetragonal phase is illustrated in Fig. 1. The molecules, all oriented in the same direction, form linear chains parallel to the c axis. The tetragonal and orthorhombic structures differ by a slight distortion in the (001) plane. Neutron-diffraction measurements³ have shown that the (001) plane changes from a 0.463-nm square to a 0.410×0.480 -nm² rectangle between these phases.

Raman spectra have been reported for the liquid and solid hydrogen cyanide at ambient pressure.⁴ The C—H stretching frequency decreases significantly at the freezing point, clearly indicating that N \cdots H—C bonds form among the linearly aligned molecules in the crystals. Only one lattice mode, a libration, has been detected in Raman spectra of the solids. Although the symmetry-imposed degeneracy of the librations of the tetragonal phase is lifted in the orthorhombic phase, no splitting by the anisotropic crystal field has been observed. This libration is split, however, into transverse-optical (TO) and longitudinal-optical (LO) components by coupling between the librations of these very polar molecules and the resulting macroscopic electric field.^{4,5} The LO-TO splitting is large, in wave numbers about 70 cm^{-1} , for both solid phases, reflecting the high polarity of hydrogen cyanide.

Because the molecular and crystal structures are sim-

ple, several theoretical studies have been made of the structures and vibrations of hydrogen cyanide.^{6–8} Rae has successfully modeled the lattice energies of these structures at ambient pressures and computed dimensions of the tetragonal and orthorhombic structures in good agreement experimental values by minimizing the lattice energy.⁶ His lattice-dynamical calculations also showed that the tetragonal-orthorhombic transition could be associated with an instability in the transverse-acoustic (TA) branch.⁹ “Softening” of the TA mode associated with the transition was later observed by neutron scattering.¹⁰ The Raman intensity and LO-TO splitting of the librational mode have been calculated by Munn using effective polarizabilities of the hydrogen cyanide molecule,¹¹ and volumes comparable to the experimental volumes have been computed by treating hydrogen cyanide as three point charges centered on the nuclei.

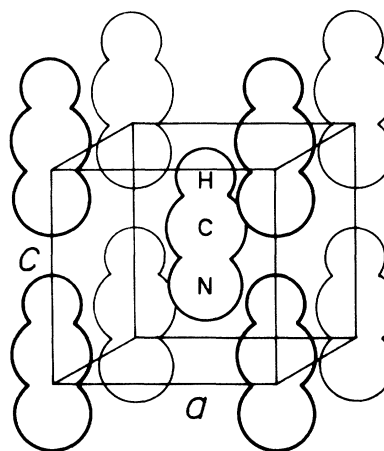


FIG. 1. The crystal structure of body-centered tetragonal hydrogen cyanide (adapted from Ref. 2).

High-pressure data are of great use for examining or constructing theoretical models for molecular solids. Thus, in this first study of hydrogen cyanide at high pressures, we used Raman spectroscopy to investigate phase transitions and vibrations. Phase and chemical transitions induced under pressure and changes of the LO-TO splitting of the librational mode will be discussed in terms of the observed Raman spectra.

EXPERIMENTAL

Safety considerations: Hydrogen cyanide is extremely toxic and may react explosively.¹²

Liquid hydrogen cyanide (99.5% pure) was obtained commercially (Fumico, Inc., Texas). During these experiments, the hydrogen cyanide was confined to a stainless-steel tank in which it was supplied, a glove box with a volume greater than 200 liters, purged with flowing dry nitrogen inside a high-velocity exhaust hood in a controlled-access laboratory, or a gasketed diamond-anvil cell designed for Raman spectroscopy.¹³ The tank of liquid hydrogen cyanide was sealed with two valves.

The diamond-anvil cell, gasket, and sapphire chips for pressure measurements were prepared for loading in ways we have used for other cryogenic materials.¹⁴ The cell was then sealed in the glove box with the cylinder of liquid hydrogen cyanide and a Dewar of liquid nitrogen, and the glove box was purged with dry nitrogen gas to remove water that might initiate polymerization of liquid hydrogen cyanide. The diamond-anvil cell was then cooled with liquid nitrogen to a temperature about 20 K below the melting point of hydrogen cyanide. During cooling, the temperature of the cell was monitored with a thermocouple inserted into the body of the cell.

When the diamond-anvil cell was at the desired temperature, the main valve on the hydrogen cyanide cylinder was carefully opened to admit a small amount of liquid (less than 0.5 ml) into the tubing between the two valves. The main valve was then closed, and the second valve was carefully opened to allow a drop or two (a few microliters) of liquid to fall on the metal gasket. The liquid immediately froze into the gasket hole to become a transparent solid. The cell was then quickly closed to trap the hydrogen cyanide. The sealed cell was left in the glove box for the next hour and allowed to warm to ambient temperature, while the excess hydrogen cyanide, highly diluted by nitrogen, was swept from the glove box and vented up the hood.

When we used the 515-nm light from an argon-ion laser to excite Raman spectra of the hydrogen cyanide, we damaged the sample, even with laser powers in the few milliwatt range. That is, the transparent sample gradually turned brown, presumably by a photopolymerization reaction. Thus, Raman spectra reported here were excited with monochromatic light near 610 nm from a Spectra-Physics 365 rhodamine-6G dye laser tuned with a triple-birefringent filter. The excitation was focused to a relatively large spot, about 0.4 mm in diameter, and the incident power was kept to a few tens of milliwatts to avoid heating the sample. With the red excitation, neither chemical reactions nor color changes were

detected. The scattered light was collected in a back-scattering geometry and analyzed through a Spex 1400 double monochromator with photon-counting detection. We determined the pressure in the hydrogen cyanide from the peak shift of the ruby R_1 luminescence, using a pressure coefficient of $7.53 \text{ cm}^{-1} \text{ GPa}^{-1}$. All measurements were made at ambient temperature, $293 \pm 3 \text{ K}$.

RESULTS

Hydrogen cyanide froze into a tetragonal phase at 0.2 GPa and further transformed into an orthorhombic phase at 0.8 GPa. Freezing was detected while the pressure was being increased, when crystallization of small grains turned the transparent liquid suddenly opaque at 0.2 GPa. A single crystal was easily prepared from the liquid by carefully controlling the pressure during freezing. Its shape was rectangular or lenticular, depending on the orientation of the growing crystal faces. This high-pressure phase was identified with the low-temperature tetragonal phase from the observed Raman spectra.⁴

Visual observations with a microscope provided no evidence for a solid-solid transition between 0.2 and 1.3 GPa. However, Raman spectra revealed that the tetragonal hydrogen cyanide transformed to orthorhombic hydrogen cyanide at 0.8 GPa in correspondence with the low-temperature structural sequence. Above 1.3 GPa, the transparent crystal gradually turned red and finally black, even in the dark. Infrared spectra of the reaction product, recovered at ambient pressure, suggest the formation of a conjugated linear polymer.¹⁵

Figure 2 shows Raman spectra of the tetragonal phase at 0.3 GPa and the orthorhombic phase at 1.3 GPa. One strong broad peak was observed in the low-wave-number region, around 140 cm^{-1} . At higher wave numbers, a strong sharp peak appeared near 2100 cm^{-1} ; and a weak broad peak occurred near 3150 cm^{-1} . We assigned these peaks as the librational, $\text{C}\equiv\text{N}$ stretching, and $\text{C}-\text{H}$ stretching modes in order of increasing frequency, following vibrational assignments in the literature.⁴ The inter-

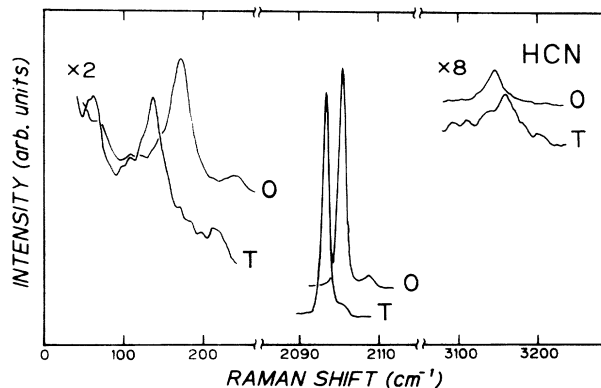


FIG. 2. Raman spectra of (lower spectrum) tetragonal hydrogen cyanide at 0.3 GPa and (upper spectrum) orthorhombic hydrogen cyanide at 1.1 GPa. Both spectra were recorded at ambient temperature.

nal bending peak was not detected in these high-pressure spectra; it probably was hidden in the background noise. Near 0.8 GPa, the overall spectral profiles for the two phases were very similar. The degeneracy of the librational peak is lifted in the orthorhombic phase; however, the correlation splitting of the librational peak was not resolved until higher pressures (see below). Additional weak LO peaks were detected on the high-wave-number sides of the TO bands for the librational and $C\equiv N$ stretching modes. The LO-TO splitting of the librational mode was as large as 70 cm^{-1} , while that of the $C\equiv N$ stretching mode was only 5 cm^{-1} .

The profile of the $C\equiv N$ stretching band varied from sample to sample, depending upon crystal orientation. Figure 3 shows Raman spectra of two single crystals grown in the diamond-anvil cell. The LO peak, which is clearly evident at 2103 cm^{-1} in the upper spectrum, is absent in the lower spectrum. In the back-scattering geometry, the LO component of the stretching mode is inactive for crystals whose c axes are parallel to the culets of the diamond anvils, such as the one used to collect the lower spectrum of Fig. 3. For polycrystalline samples,⁴ the LO peak appeared as a broad tail of the TO band, instead of a distinct peak, as a consequence of averaging contributions of randomly oriented small crystals to the Raman scattering.⁹

The wave-numbers of the librational Raman bands are plotted versus pressure to 1.3 GPa in Fig. 4. The wave numbers of both the TO and LO bands increase rapidly with pressure, and the rates of increase distinctly change at 0.8 GPa, becoming much greater above that pressure. These changes in the wave-number–pressure relation are caused by the tetragonal-to-orthorhombic phase transition.

The LO-TO splitting of the librational mode decreased with increasing pressure from 78 cm^{-1} at 0.2 GPa, by

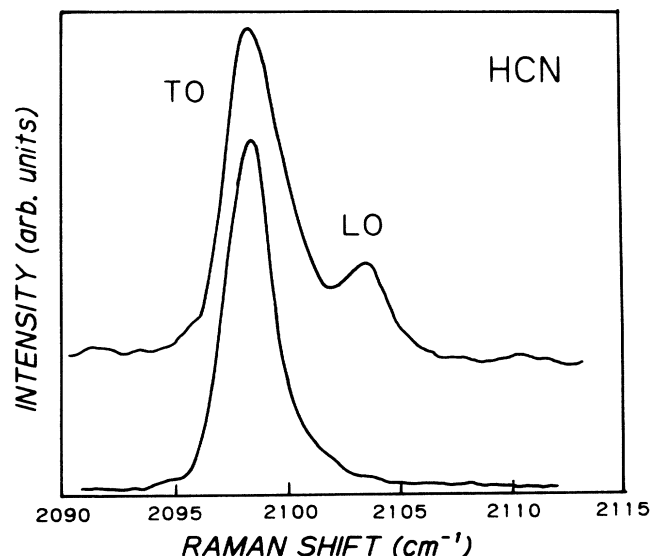


FIG. 3. Raman spectra of the $C\equiv N$ stretching mode for two crystalline orientations.

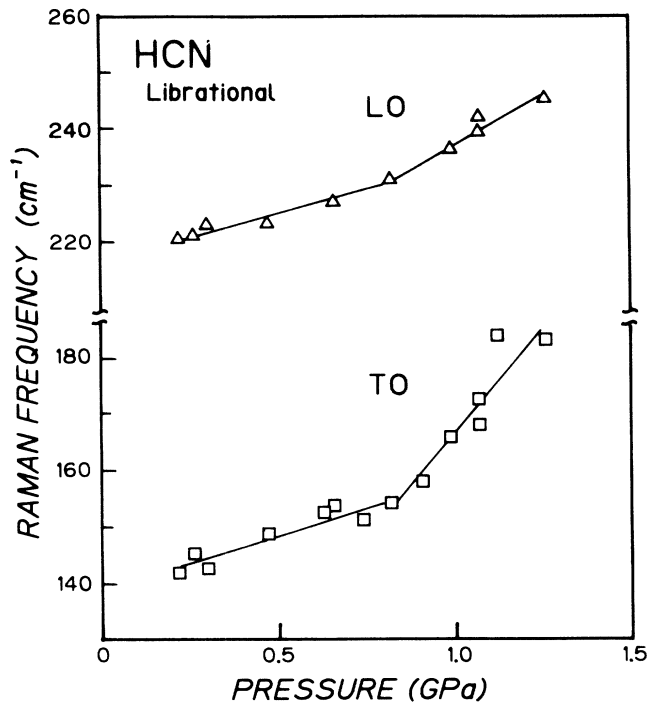


FIG. 4. Pressure dependences of the wave numbers of the Raman shifts of the TO and LO librational modes.

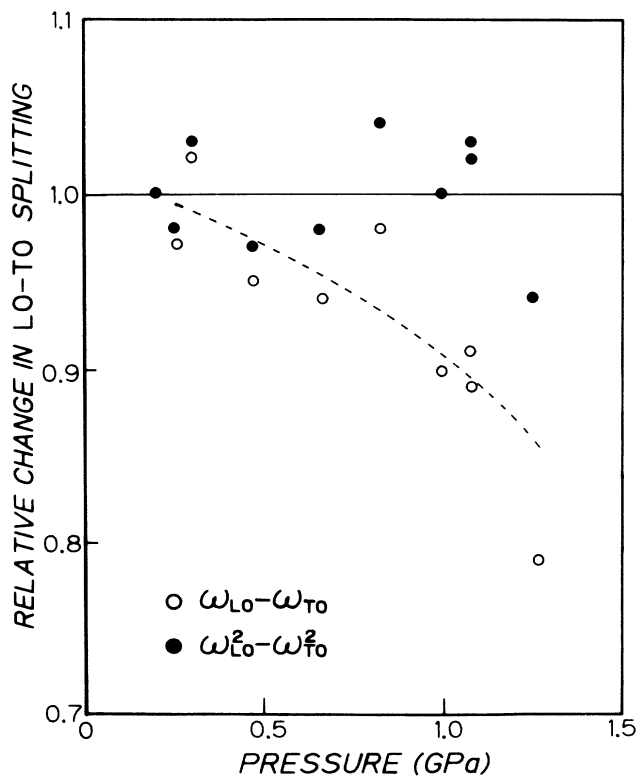


FIG. 5. $\omega_{LO}-\omega_{TO}$ and $\omega_{LO}^2-\omega_{TO}^2$, relative to values of these differences at 0.2 GPa, vs pressure for the librational mode of solid hydrogen cyanide.

$-10 \text{ cm}^{-1} \text{ GPa}^{-1}$ in the tetragonal phase, and $-30 \text{ cm}^{-1} \text{ GPa}^{-1}$ in the orthorhombic phase. At 1.3 GPa, the splitting was only 62 cm^{-1} . These changes are very large compared to pressure dependences of the LO-TO splittings of zinc-blende III-V semiconductors like indium antimonide.^{16,17} The largest pressure coefficient for these compounds, $-0.92 \text{ cm}^{-1} \text{ GPa}^{-1}$ for aluminum nitride, is an order of magnitude smaller than that of hydrogen cyanide. Figure 5 shows the relative changes with pressure of the LO-TO splitting, $\omega_{\text{LO}} - \omega_{\text{TO}}$, and, for purposes of discussion, $\omega_{\text{LO}}^2 - \omega_{\text{TO}}^2$. In contrast to the decrease of $\omega_{\text{LO}} - \omega_{\text{TO}}$, $\omega_{\text{LO}}^2 - \omega_{\text{TO}}^2$ is virtually constant.

Figure 6 shows how the wave numbers of the internal modes vary with pressure. The position of the $\text{C}\equiv\text{N}$ stretching band remains virtually constant, while the wave number of the $\text{C}-\text{H}$ stretching band decreases with increasing pressure by about $-13 \text{ cm}^{-1} \text{ GPa}^{-1}$. This value is similar to the rate of decrease of the wave number of the $\text{C}-\text{H}$ stretching mode of solid cyanoacetylene¹⁸ in which HCCCN molecules are also aligned in linear chains by $\text{N}\cdots\text{H}-\text{C}$ hydrogen bonds.

At higher pressures, a shoulder began to develop on the low-wave-number side of the librational TO band. Figure 7 shows this shoulder to be a spectrum of orthorhombic hydrogen cyanide at 1.3 GPa. This band was deconvoluted into two peaks at 174 and 186 cm^{-1} by a curve-fitting procedure. The appearance of this shoulder is consistent with the symmetry-allowed splitting of the librations of orthorhombic hydrogen cyanide. At this temperature and lower pressures, this splitting was not resolved, presumably because it was too small relative to the width of the band.

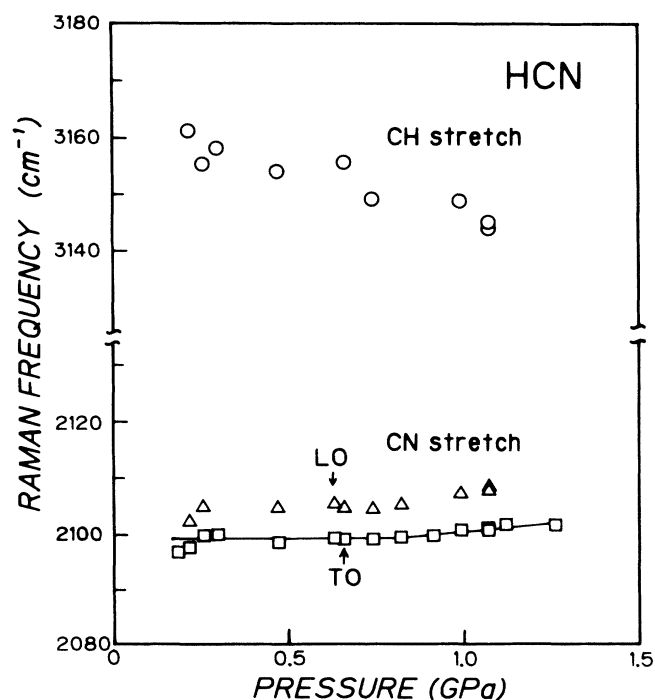


FIG. 6. Pressure dependences of the wave numbers of the Raman shifts of the $\text{C}-\text{H}$ and $\text{C}\equiv\text{N}$ stretching modes.

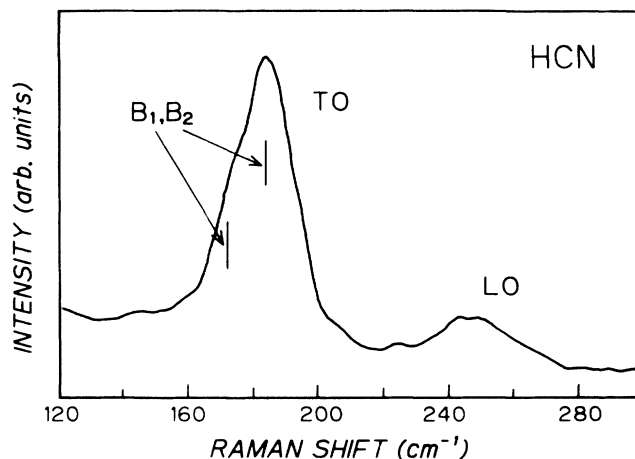


FIG. 7. The Raman spectrum in the region of the hydrogen cyanide librational mode at 1.3 GPa and ambient temperature.

DISCUSSION

We have measured Raman spectra of tetragonal and orthorhombic hydrogen cyanide at pressures from 0.2 to 1.3 GPa. Characteristic pressure dependences observed for the internal and librational modes are (1) a large decrease of the $\text{C}-\text{H}$ stretching frequency, (2) a very slight increase of the $\text{C}\equiv\text{N}$ stretching frequency, (3) large increases of the TO librational frequency, which splits into two components in orthorhombic hydrogen cyanide at 1.3 GPa, and (4) the TO-LO splitting of the librational band varies such that $\omega_{\text{LO}}^2 - \omega_{\text{TO}}^2$ stays nearly constant. The discussion interprets changes of the chemical bonds and structures of these hydrogen cyanide crystals in terms of these high-pressure Raman spectra.

Internal modes

The sign and size of the pressure dependence of the $\text{C}-\text{H}$ stretching frequency, $-13 \text{ cm}^{-1} \text{ GPa}^{-1}$, implies that the motion of the hydrogen atoms is strongly influenced by hydrogen bonding in the molecular chain and the strength of the $\text{N}\cdots\text{H}-\text{C}$ bond between a H atom and the neighboring N atom increases as solid hydrogen cyanide is compressed. Since the hydrogen atoms are essentially buried within the chains, other nearby molecules have negligible effects on the movements of the H atoms. Similar effects of pressure on internal modes of hydrogen-bonded solids have been observed for cyanoacetylene,¹⁹ ammonium chloride,²⁰ water,²¹ and alcohols.²² In the high-pressure solid phase,^{18,19} cyanoacetylene molecules align by $\text{N}\cdots\text{H}-\text{C}$ hydrogen bonds into infinite linear chains like those of hydrogen cyanide. The pressure dependence of the $\text{C}-\text{H}$ stretching mode of cyanoacetylene, $-15 \text{ cm}^{-1} \text{ GPa}^{-1}$, is similar to that of hydrogen cyanide.¹⁹ The other internal stretching motion, the $\text{C}\equiv\text{H}$ stretch, shifted only slightly to higher frequency.

Double-well potential models provide a qualitative explanation for the "softening" of the $\text{C}-\text{H}$ stretching frequency of these bonds.²³ If the potential for the motion

of the H atom along the chain is approximated by a deep well with a minimum on the side of the C atom (C site) and a relatively shallow well on the side of the N atom (N site), the H atom will vibrate around an equilibrium position in the C-site well with a frequency predominantly determined by the curvature at the potential minimum, the C site. As the chain is compressed, the two wells increasingly overlap; the curvature at the C site decreases;²³ and the C—H stretching frequency decreases. Extension of this qualitative double-well model suggests that the C—H bond lengthens as the overlap of the two wells increase; however, more detailed calculations contradict this conclusion.²⁴ When the high-pressure behavior of an isolated chain of hydrogen cyanide molecules was modeled by *ab initio* molecular-orbital methods, the frequency of the hydrogen-bonded C—H stretching vibration was calculated to decrease when the molecular chain was compressed. However, the length of the C—H bond was also calculated to decrease. Further theoretical studies are required to understand the pressure dependence of the hydrogen bond in solid hydrogen cyanide.

Librational mode

The shifts of the librational modes provide interesting insights about intermolecular interactions in solid hydrogen cyanide and the nature of the tetragonal-to-orthorhombic transition. The orthorhombic distortion of the tetragonal structure varies the ratio of the lengths of the axes in the (001) plane, b/a , from unity. This axial ratio is a useful parameter for describing the transition.

The virtually continuous shifts of the frequencies of the Raman-active libration and internal vibrational modes between 0.2 and 1.3 GPa suggests that the tetragonal-to-orthorhombic transition has second-order character at 0.8 GPa and ambient temperature. This behavior is very different from what is reported at ambient pressure. At 170 K and 0.1 MPa, the first-order character of the tetragonal-to-orthorhombic transition is obvious from both the abrupt change in the b/a ratio from unity to 1.15³ and 12- and 16-cm⁻¹ shifts of the wave numbers of the libration and C—H stretching vibration, respectively.⁴ The fact that, at ambient temperature, the B_1 - B_2 splitting of the libration was resolved only at 1.3 GPa, 0.5 GPa above the transition pressure, also suggests that the transition occurs more gradually at the higher temperature. Thus, there may be a tricritical point on the tetragonal-to-orthorhombic boundary between ambient pressure and 1.3 GPa.

The increase in the b/a ratio under pressure is naturally expected from the viewpoint of increasing the packing fraction of linear chains. In the tetragonal structure with $b/a=1$, each molecular chain has four equivalent first neighbors at a distance $a/\sqrt{2}$ and four equivalent second neighbors at a distance a ; see Fig. 1. For the orthorhombic structure with $b/a \neq 1$, the four second-neighboring chains of the tetragonal structure are rearranged into two second and two third neighbors. As b/a increases, the distances to the four first- and two second-neighbor chains approach each other. When $b/a = \sqrt{3}$, these six distances become equal, and the arrangement of chains

has hexagonal symmetry, if the molecular displacements along the c axis are neglected. The gradual increase of b/a with increasing pressure is interpreted as a transitional process from a loosely packed four-coordinate structure to a close-packed six-coordinate structure. Nearly close-packed hexagonal lattices of linear molecular chains are known at ambient pressure for cyanoacetylene¹⁸ and its halogen derivatives such as chloroacetylene.²⁵

The fact that the orthorhombic distortion effectively increases the coordination number of a given molecular chain, and thus the effective number of near neighbors that are being compressed around a chain, is consistent with the observation that the rate of increase of the librational frequency with pressure is greater in the orthorhombic phase. Two kinds of short-range interactions arise from the increased overlapping of molecular orbitals when hydrogen cyanide chains are compressed together, exchange and penetration-Coulomb interactions.⁶ Exchange interactions increase the lattice energy, and penetration-Coulomb interactions lower the energy of the lattice. Rae calculated the lattice energy for both the tetragonal and orthorhombic structures and obtained cell dimensions in good agreement with experimental values by minimizing the lattice energy with respect to the cell parameters. He also showed that the increase of the lattice energy contributed by the exchange terms is the more important effect of compressing and distorting the a and b axes. The lattice energy rises sharply as the chains approach each other, and the curvature at the potential minima increases. Thus, the increase of the librational frequencies is a sensitive, qualitative measure of the degree of compression in the basal plane.

LO-TO splitting

The pressure dependence of the LO-TO splitting of the librational mode is also interesting. As shown in Fig. 5, the difference between the squares of the LO and TO frequencies, $\omega_{\text{LO}}^2 - \omega_{\text{TO}}^2$, varied little with pressure. One interpretation for this pressure- or volume-independent behavior is provided by theoretical modes that compute the LO-TO splitting using an effective polarizability of the hydrogen cyanide molecule.¹¹ This model describes the LO-TO splitting in the orthorhombic crystal by

$$\omega_{\text{LO}}^2 - \omega_{\text{TO}}^2 = (\mu/I\epsilon_0 V)(\partial P_a / \partial \theta_b), \quad (1)$$

where ϵ_0 is the permittivity of free space, V is the volume of the primitive unit cell, I is the moment of inertia of the molecule, μ is the effective dipole moment of the molecule, P_a is the component along the \mathbf{a} axis of the effective dipole associated with libration about the \mathbf{b} axis, and θ_b is the angle of rotation around the \mathbf{b} axis.¹¹ Two terms on the right-hand side of (1), V and $\partial P_a / \partial \theta_b$, depend upon volume and, therefore, pressure. The volume independence of $\omega_{\text{LO}}^2 - \omega_{\text{TO}}^2$ observed experimentally implies that the effects of these two terms cancel. This observation can then be used to compute the volume or pressure dependence of the TO-LO splitting.

SUMMARY

This Raman study of crystalline hydrogen cyanide has provided interesting results regarding pressure changes in the chemical bonds and structures of these crystals. They are the strengthening of the hydrogen bond, the gradual nature of the structural distortion towards close-packing at ambient temperature, and the pressure-independent behavior of the TO-LO splitting in terms of $\omega_{LO}^2 - \omega_{TO}^2$. We have discussed the frequency shifts and peak profiles on the basis of anisotropic structural changes in the orthorhombic phase that were inferred from the Raman results. Structural studies of hydrogen cyanide by x-ray or

neutron diffraction to pressures of the order of 1.3 GPa and further computational analysis are needed to develop the qualitative understanding of the nature of hydrogen cyanide crystals at high pressures on firmer quantitative grounds.

ACKNOWLEDGMENTS

We are grateful for financial support from The National Science Foundation (NSF) Grant No. DMR 87-14897, Los Alamos National Laboratory-Institute of Geophysics and Planetary Physics Grant No. 194 (H.C.C.), and Lawrence Livermore National Laboratory-Institute of Geophysics and Planetary Physics Grant No. 90-02 (B.J.B.).

*Permanent address: National Chemical Laboratory for Industry, Tsukuba Research Center, Tsukuba, Ibaraki 305, Japan.

¹W. F. Giauque and R. A. Ruehrwein, *J. Amer. Chem. Soc.* **61**, 2626 (1939).

²W. J. Dulmage and W. N. Lipscomb, *Acta Crystallogr.* **4**, 330, (1951).

³O. W. Dietrich, G. A. Mackenzie, and G. S. Pawley, *J. Phys. C* **8**, L98 (1975).

⁴M. Pezolet and R. Wavoie, *Can. J. Chem.* **47**, 3041 (1969).

⁵P. F. Krause and H. B. Friedrich, *J. Chem. Phys.* **76**, 1140 (1972).

⁶A. I. M. Rae, *Mol. Phys.* **16**, 257 (1969).

⁷M. Kertesz, J. Koller, and A. Azman, *Chem. Phys. Lett.* **41**, 146 (1976).

⁸P. L. Cummins, G. B. Backs, N. S. Hush, and B. Jonsson, *Chem. Phys. Lett.* **145**, 399 (1988).

⁹A. I. M. Rae, *J. Phys. C* **5**, 3309 (1972).

¹⁰G. A. Mackenzie and G. S. Pawley, *J. Phys. C* **12**, 2717 (1979).

¹¹R. W. Munn, *Chem. Phys.* **59**, 269 (1981).

¹²National Research Council-Committee on Hazardous Substances in the Laboratory, *Prudent Practices for Handling Hazardous Chemicals in Laboratories* (National Academy, Washington, 1981).

¹³K. R. Hirsch and W. B. Holzapfel, *Rev. Sci. Instrum.* **52**, 52 (1981).

¹⁴B. J. Baer and M. Nicol, *J. Phys. Chem.* **93**, 1683 (1989).

¹⁵K. Aoki, B. J. Baer, H. C. Cynn, and M. Nicol (unpublished).

¹⁶J. A. Sanjurjo, E. Lopez-Crus, P. Vogl, and M. Cardona, *Phys. Rev. B* **28**, 4579 (1983).

¹⁷K. Aoki, E. Anastassakis, and M. Cardona, *Phys. Rev. B* **30**, 681 (1984).

¹⁸F. V. Shallcross and G. B. Carpenter, *Acta Crystallogr.* **11**, 490 (1958).

¹⁹K. Aoki, Y. Kakudate, M. Yoshida, S. Usuba, and S. Fujiwara, *J. Chem. Phys.* **91**, 2814 (1989).

²⁰Y. Ebisuzaki and M. Nicol, *Chem. Phys. Lett.* **3**, 480 (1969).

²¹W. B. Holzapfel, B. Seiler, and M. Nicol, *J. Geophys. Res.* **89**, Suppl. B707 (1984).

²²J. F. Mammone, S. K. Sharma, and M. Nicol, *J. Phys. Chem.* **84**, 3130 (1980).

²³R. W. Jansen, R. Bertoni, D. A. Pinnick, A. I. Katz, R. C. Hanson, O. F. Sankey, and M. O'Keeffe, *Phys. Rev. B* **35**, 9830 (1987).

²⁴T. Matsunaga, K. Aoki, S. Fujiwara, and K. Tanaka (unpublished).

²⁵T. Bjorvatten, *Acta Chem. Scand.* **22**, 410 (1968).